Physica D 47 (1991) 393–415
North-Holland

STABILITY OF ISOTROPIC SINGULARITIES FOR THE NONLINEAR SCHRÖDINGER EQUATION

M.J. LANDMAN[a], G.C. PAPANICOLAOU[a], C. SULEM[b], P.L. SULEM[c] and X.P. WANG[a]
[a]*Courant Institute of Mathematical Sciences, 251 Mercer Street, New York, NY 10012, USA*
[b]*CNRS, ENS-CMA, 45 rue d'Ulm, Paris 75230, France and Toronto University, Toronto MSSIAI, Canada*
[c]*CNRS, Observatoire de Nice, B.P. 139, 06003 Nice, France*
and School of Mathématical Sciences, Tel-Aviv University, 69978 Tel-Aviv, Israel

Received 12 February 1990
Revised manuscript received 5 June 1990
Accepted 16 June 1990
Communicated by A.C. Newell

We describe a method by which the fully two- and three-dimensional cubic Schrödinger equations can be accurately integrated numerically up to times very close to the formation of singularities. In both cases, anisotropic initial data collapse very rapidly towards isotropic singularities. In three dimensions, the solutions become self-similar with a blowup rate $(t^*-t)^{-1/2}$. In two dimensions, the self-similarity is weakly broken and the blowup rate is $[(t^*-t)/\ln\ln 1/(t^*-t)]^{-1/2}$. The stability of the singular isotropic solutions is very firmly backed by the numerical results.

1. Introduction

The nonlinear Schrödinger equation (NLS) with cubic nonlinearity

$$\begin{aligned} &i\psi_t + \Delta\psi + |\psi|^2\psi = 0 \quad t > 0, \\ &\psi(0,x) = \psi_0(x) \qquad x \in \mathbb{R}^d, \end{aligned} \tag{1.1}$$

arises in various physical contexts as an amplitude equation for weakly nonlinear waves [1]. For a certain class of initial conditions, namely those for which the invariant $H = \int_0^t (|\nabla\psi|^2 - \frac{1}{2}|\psi|^4)\,dx$ is negative, the NLS has solutions that become singular in a finite time when the dimension of the space d is larger than or equal to two [2, 3]. In refs. [4, 5], we studied numerically the local form of the singularity, restricted to isotropic solutions. In order to compute numerically radially symmetric solutions of the nonlinear Schrödinger equation up to times very close to blowup, we introduced the method of dynamic rescaling. A time-dependent change of variables is done on the amplitude of the solution, on the (radial) space variable and on time. The scaling factors are chosen to preserve integral norms of the derivatives of the solution in the transformed variables. In this way the transformed solutions remain smooth and the nature of the singularity of the original solutions can be determined from the asymptotic behavior of the scale factor. We found that in the supercritical case $d > 2$, the singular solutions have a blowup rate $(t^*-t)^{-1/2}$ and a self-similar character of the form predicted by Zakharov [8],

$$\psi(x,t) = \frac{1}{\sqrt{2K(t^*-t)}}\,Q\left(\frac{|x|}{\sqrt{2K(t^*-t)}}\right) e^{(i/2K)\log[t^*/(t^*-t)]} \tag{1.2}$$

where Q satisfies the ordinary differential equation

$$Q_{\xi\xi} + \frac{d-1}{\xi} Q_\xi - Q + iK(\xi Q)_\xi + |Q|^2 Q = 0, \quad Q_\xi(0) = 0, \quad Q(0) \text{ is real}, \quad Q(\infty) = 0. \tag{1.3}$$

We also obtained precise estimates for the constant K. In dimension $d = 3$, $K \approx 0.9173$. Note that in the supercritical case $d > 2$, the asymptotic form of the blowup rate is reached very early and can thus be observed in direct numerical simulations [5, 7].

A similar dynamic rescaling method but without amplitude rescaling has recently been used in ref. [9]. However, instead of solving the rescaled equation in the entire space, these authors consider a finite domain, using an approximate boundary condition based on the large-distance behavior of the solution as given in ref. [5]. This method allows substantial reduction of the spatial domain of integration.

In the critical case $d = 2$, a dynamical mesh refinement is essential to reach the asymptotic regime. Our calculations [4] suggest that self-similarity is weakly violated and that the previous blowup rate must be corrected by a function varying slower than a logarithm. In refs. [10, 11] (see also ref. [12]) we showed by a perturbation method with respect to the space dimension that the blowup rate is $[(t^* - t)/\ln\ln 1/(t^* - t)]^{-1/2}$. We were later informed that this result was obtained by Fraiman [13] on a more physical basis.

In this paper we extend the dynamic rescaling idea to anisotropic solutions so that we can follow the evolution towards the formation of singularities of initial data $\psi_0(x)$ that are not radially symmetric. However, we assume that $|\psi_0(x)|$ blows up at only one point. We are then able to track dynamically the solution in a new set of coordinates that allows for scaling, rotation and translation of the axes. Details on the method are given in section 2. In the transformed variables, solutions of the NLS remain regular. The behavior of the scale factors in different directions determines the rates of collapse in these directions and thus the nature of the singularity in the original variables. The anisotropic dynamic rescaling gives a way to accurately detect the possible anisotropic collapse of the solutions. The numerical method is described in section 3. We implement a boundary condition similar to that used in ref. [9]. In the two- and three-dimensional problems, this approximation is essential in order to reduce the size of the spatial domain over which the solution is calculated.

The main results of our computation both in two and three dimensions are presented in section 4. We find that the isotropic singular solutions are dynamically stable with respect to a broad class of anisotropic initial perturbations. In both cases, anisotropic initial data collapse very rapidly towards the isotropic singularities. In the last section we compare our results based on the dynamic mesh refinement method with results obtained previously.

2. Anisotropic dynamic rescaling

We introduce a general change of dependent and independent variables in the nonlinear Schrödinger equation (1.1) in dimension d. Let $D(t)$ be a $d \times d$ matrix function of time, $x_0(t)$ a vector function of time and $L(t)$ a nonnegative scalar function. We consider a change of variables

$$\xi = D^{-1}(t)(x - x_0), \qquad \tau = \int_0^t \frac{1}{L^2(s)}\, ds, \qquad u(\xi, \tau) = L(t)\psi(x, t), \tag{2.1}$$

where the matrix $D(t)$ has the form

$$D(t) = O^{\mathrm{T}}(t)\Lambda(t), \tag{2.2}$$

with $O(t)$ an orthogonal matrix and $\Lambda(t)$ a diagonal matrix whose diagonal elements are λ_i $(i = 1, \ldots, d)$. We will choose $D(t)$, $L(t)$ and $x_0(t)$ so that the transformed solution u has desirable properties, such as boundedness.

Substituting (2.1) into (1.1) and noting that $D^{\mathrm{T}}D = \Lambda^2$, the NLS becomes

$$\mathrm{i}\left[u_\tau - L^{-1}L_\tau u + f\cdot\nabla u\right] + L^2(\Lambda^{-2}:\nabla\nabla)u + |u|^2u = 0, \tag{2.3}$$

where

$$f = -D^{-1}\frac{\mathrm{d}D}{\mathrm{d}\tau}\xi - D^{-1}\frac{\mathrm{d}x_0}{\mathrm{d}\tau}$$

and

$$\nabla\nabla = \left(\frac{\partial^2}{\partial\xi_i\,\partial\xi_j}\right), \quad i, j = 1, \ldots, d.$$

The matrix product : is defined by

$$A:B = \sum_{i,j=1}^{d} a_{ij}b_{ij} \quad \text{where } A = (a_{ij}),\ B = (b_{ij}).$$

Note that we may consider L, D and x_0 as functions of t or as functions of τ, because of (2.1). These quantities can be chosen in several ways. One choice is so that the transformed solution is as close as possible to isotropy. Let p be a positive integer. We take x_0 to be the centroid of $2p$ power of $|\psi|$, which, for large τ, is very likely to be the blowup point

$$x_0^i = \frac{\int x_i|\psi|^{2p}\,\mathrm{d}x}{\int|\psi|^{2p}\,\mathrm{d}x}. \tag{2.4}$$

We will use $p \geq 3$ in order to ensure accuracy in the numerical computation of the integrals. To make u as isotropic as possible we choose $D(t)$ so that the second moment of $|u|^{2p}$ is the identity matrix, i.e.

$$\frac{\int\xi_i\xi_j|u|^{2p}\,\mathrm{d}\xi}{\int|u|^{2p}\,\mathrm{d}\xi} = \delta_{ij} \tag{2.5}$$

or, using (2.1),

$$D^{-1}S(D^{-1})^{\mathrm{T}} = I, \tag{2.6}$$

where $S = (s_{ij})$ and

$$s_{ij} = \frac{\int (x^i - x_0^i)(x^j - x_0^j)|\psi|^{2p}\,\mathrm{d}\boldsymbol{x}}{\int |\psi|^{2p}\,\mathrm{d}\boldsymbol{x}}. \tag{2.7}$$

We also set

$$L(t) = \sqrt{\frac{d}{\Sigma 1/\lambda_i^2}}, \tag{2.8}$$

which makes the coefficients of the second-order derivative terms in (2.3) bounded by 1.

Given ψ, we compute S from (2.7) and (2.4). Since S is symmetric and positive definite we have the decomposition $S = O^{\mathrm{T}}\Lambda^2 O$. If S has distinct eigenvalues (i.e. ψ is anisotropic) then O is unique.

To see how $\boldsymbol{x}_0, D, L$ vary with time, we take the derivatives of (2.4), (2.6)–(2.8) with respect to the scaled time τ. Taking the derivative of (2.4) and using (1.1) and (2.1) we get

$$\frac{\mathrm{d}\boldsymbol{x}_0}{\mathrm{d}\tau} = 2D\boldsymbol{\beta}, \tag{2.9}$$

where $\boldsymbol{\beta} = (\beta_j)$ $(j = 1, \ldots, d)$ and

$$\beta_j = \frac{p\int \xi_j |u|^{2(p-1)} \mathrm{Im}(L^2\Lambda^{-2} : u\nabla\nabla)u^*\,\mathrm{d}\boldsymbol{\xi}}{\int |u|^{2p}\,\mathrm{d}\boldsymbol{\xi}}. \tag{2.10}$$

Differentiating (2.7) and using (1.1) and (2.1) gives

$$\frac{\mathrm{d}S}{\mathrm{d}\tau} = -2DAD^{\mathrm{T}}, \tag{2.11}$$

where $A = (a_{ij})$ $(i, j = 1, \ldots, d)$ with

$$a_{ij} = \frac{p\int (\delta_{ij} - \xi_i\xi_j)|u|^{2(p-1)} \mathrm{Im}(L^2\Lambda^{-2} : u\nabla\nabla)u^*\,\mathrm{d}\boldsymbol{\xi}}{\int |u|^{2p}\,\mathrm{d}\boldsymbol{\xi}}. \tag{2.12}$$

But from (2.6), $S = DD^{\mathrm{T}} = O^{\mathrm{T}}\Lambda^2 O$, so that we have

$$\frac{\mathrm{d}S}{\mathrm{d}\tau} = \frac{\mathrm{d}}{\mathrm{d}\tau}(DD^{\mathrm{T}}) = \dot{O}^{\mathrm{T}}\Lambda^2 O + 2O^{\mathrm{T}}\Lambda\dot{\Lambda}O + O^{\mathrm{T}}\Lambda^2\dot{O},$$

i.e.

$$O\dot{S}O^{\mathrm{T}} = O\dot{O}^{\mathrm{T}}\Lambda^2 + 2\Lambda\dot{\Lambda} + \Lambda^2\dot{O}O^{\mathrm{T}}, \tag{2.13}$$

where the dot means the derivative with respect to τ. Then, using (2.11) we have

$$-2\Lambda A\Lambda = O\dot{O}^{\mathrm{T}}\Lambda^2 + 2\Lambda\dot{\Lambda} + \Lambda^2\dot{O}O^{\mathrm{T}}. \tag{2.14}$$

From this equation, we can derive a system of decoupled evolution equations for Λ and O. Set

$$O\dot{O}^{\mathrm{T}} = G = (g_{ij}), \tag{2.15}$$

which is skew-symmetric, so we have $g_{ii} = 0$. Equating the diagonal elements of (2.14) we get

$$\dot{\lambda}_i = -\lambda_i a_{ii}. \tag{2.16}$$

Equating the off-diagonal elements we get

$$-2\lambda_i\lambda_j a_{ij} = \lambda_j^2 g_{ij} - \lambda_i^2 g_{ij}, \tag{2.17}$$

so that

$$g_{ij} = \frac{2\lambda_i\lambda_j}{\lambda_i^2 - \lambda_j^2} a_{ij} \quad (\lambda_i \neq \lambda_j). \tag{2.18}$$

We have from (2.17), that is for $i \neq j$, $\lambda_i = \lambda_j$, then $a_{ij} = 0$ and

$$\lim_{\lambda_i \to \lambda_j} g_{ij} = \lim_{\lambda_i \to \lambda_j} \frac{2\lambda_i\lambda_j}{\lambda_i^2 - \lambda_j^2} a_{ij}.$$

It follows then from (2.15) that

$$\frac{\mathrm{d}O}{\mathrm{d}\tau} = -GO, \tag{2.19}$$

where G is given by (2.18). Finally, we derive an evolution equation for L. We take the τ derivative of (2.8) and make use of (2.16) which gives

$$\frac{1}{L}\frac{\mathrm{d}L}{\mathrm{d}\tau} = -\frac{\Sigma a_{ii}/\lambda_i^2}{\Sigma 1/\lambda_i^2}. \tag{2.20}$$

With (2.9), (2.16), (2.18) and (2.20), f in eq. (2.3) can be simplified to

$$f = -D^{-1}\frac{\mathrm{d}D}{\mathrm{d}\tau}\xi - D^{-1}\frac{\mathrm{d}x_0}{\mathrm{d}\tau} = B\xi - 2\beta,$$

where $B = (\mathrm{d}D/\mathrm{d}\tau)D^{-1} = -\dot{\Lambda}\Lambda^{-1} + \Lambda^{-1}\dot{O}O^{\mathrm{T}}\Lambda$, i.e.

$$b_{ii} = -\dot{\lambda}_i\lambda_i^{-1} = a_{ii}, \qquad b_{ij} = -\lambda_i^{-1}g_{ji}\lambda_j = \frac{2\lambda_j^2}{\lambda_j^2 - \lambda_i^2} a_{ij} \quad (i \neq j), \tag{2.21}$$

and β is given by (2.10).

In summary, we get a coupled system of evolution equations for the transformed solution u and the scaling factors λ_i,

$$\mathrm{i}\left[u_\tau - L^{-1}L_\tau u + \nabla u \cdot \boldsymbol{f}\right] + (L^2\Lambda^{-2} : \nabla\nabla)u + |u|^2 u = 0, \tag{2.22}$$

$$\frac{\mathrm{d}\lambda_i}{\mathrm{d}\tau} = -a_{ii}\lambda_i \quad (i = 1, \ldots, d). \tag{2.23}$$

Here

$$L(t) = \sqrt{\frac{d}{\Sigma 1/\lambda_i^2}}, \quad L^{-1}L_\tau = -\frac{\Sigma a_{ii}/\lambda_i^2}{\Sigma 1/\lambda_i^2}, \quad \text{and} \quad \boldsymbol{f} = B\boldsymbol{\xi} - 2\boldsymbol{\beta},$$

where B and $\boldsymbol{\beta}$ are given by (2.21) and (2.10), respectively, and (a_{ij}) is given by (2.12). We also have a system of evolution equations for the centroid of the solution $\boldsymbol{x}_0$ and the rotation matrix O,

$$\frac{\mathrm{d}\boldsymbol{x}_0}{\mathrm{d}\tau} = 2O^{\mathrm{T}}\Lambda\boldsymbol{\beta}, \tag{2.24}$$

$$\frac{\mathrm{d}O}{\mathrm{d}\tau} = -GO, \tag{2.25}$$

where G is given by (2.18).

Our first observation is that (2.22) and (2.23) are a closed system so that u and λ_i are determined by these equations alone without having to compute the rotation O or the centroid $\boldsymbol{x}_0$. This shows that the translation and rotation are not fundamental in the singularity formation. It is the local scaling that determines the collapse of the solution ψ. The secondary quantities $\boldsymbol{x}_0$ and O can be computed from (2.24) and (2.25) once u and λ_i have been obtained by solving (2.22) and (2.23).

In the radially symmetric case we have $\boldsymbol{x}_0 = 0$ and $a_{ij} = 0$ for $i \neq j$ while the a_{ii} are all equal and we denote them by $a = a_{ii}$. Therefore, $\lambda_i = \lambda$, $L = \sqrt{d/(\Sigma 1/\lambda_i^2)} = \lambda$, $L^{-1}L_\tau = -a$, and $\boldsymbol{f} = a\boldsymbol{\xi}$. Eq. (2.22) becomes

$$\mathrm{i}u_\tau + u_{\xi\xi} + \frac{d-1}{\xi}u_\xi + |u|^2 u + \mathrm{i}a(\xi u)_\xi = 0,$$

where ξ is the radial coordinate and a is given by

$$a = \frac{p\int(1-\xi^2)|u|^{2(p-1)}\mathrm{Im}(u\,\Delta u^*)\,\mathrm{d}\boldsymbol{\xi}}{\int |u|^{2p}\,\mathrm{d}\boldsymbol{\xi}}.$$

We have thus recovered the radially symmetric problem that we analyzed in refs. [3, 4].

To solve (2.25) numerically we express O in terms of the Euler angles ϕ, θ, ψ defined by

$$O = \begin{pmatrix} -\sin\phi\sin\theta + \cos\psi\cos\phi\cos\theta & \cos\phi\sin\theta + \cos\psi\sin\phi\cos\theta & -\sin\psi\cos\theta \\ -\sin\phi\cos\theta - \cos\psi\cos\phi\sin\theta & \cos\phi\cos\theta - \cos\psi\sin\phi\sin\theta & \sin\psi\cos\theta \\ \sin\psi\cos\phi & \sin\psi\sin\phi & \cos\psi \end{pmatrix}.$$

From this expression and (2.18), we obtain for $\dot{\phi}, \dot{\theta}, \dot{\psi}$,

$$\dot{\phi} = \frac{2}{\sin\psi}\left(\frac{\lambda_1\lambda_3}{\lambda_1^2-\lambda_3^2}a_{13}\sin\theta + \frac{\lambda_2\lambda_3}{\lambda_2^2-\lambda_3^2}a_{23}\cos\theta\right), \tag{2.26}$$

$$\dot{\theta} = -\frac{2\lambda_1\lambda_2}{\lambda_1^2-\lambda_2^2}a_{12} - \frac{2\cos\psi}{\sin\psi}\left(\frac{\lambda_1\lambda_3}{\lambda_1^2-\lambda_3^2}a_{13}\sin\theta + \frac{\lambda_2\lambda_3}{\lambda_2^2-\lambda_3^2}a_{23}\cos\theta\right), \tag{2.27}$$

$$\dot{\psi} = 2\left(\frac{\lambda_1\lambda_3}{\lambda_1^2-\lambda_3^2}a_{13}\cos\theta - \frac{\lambda_2\lambda_3}{\lambda_2^2-\lambda_3^2}a_{23}\sin\theta\right). \tag{2.28}$$

In two dimensions, the rotation is defined by a single angle θ,

$$O = \begin{pmatrix} \cos\theta & \sin\theta \\ -\sin\theta & \cos\theta \end{pmatrix}$$

and, making use of (2.18) again, we get

$$\dot{\theta} = -\frac{2\lambda_1\lambda_2}{\lambda_1^2-\lambda_2^2}a_{12}. \tag{2.29}$$

3. Numerical scheme and boundary conditions

In this section, we describe the numerical method we use to solve the transformed NLS equations (2.22)–(2.25). The main point is that we integrate the equations in a finite domain $\mathcal{N}=[-M, M]^d$ centered at the origin, using an approximate boundary condition. The approximate boundary conditions were also used in ref. [9] for radially symmetric problems. We extend it here to multi-dimensional problems where a reduction of the integration domain is essential to maintain accuracy at a reasonable cost. Note that the computational domain is a square in two dimensions or a cube in three dimensions and so it will be unsymmetric in the primitive variables because of the different scales in different directions.

Discretization of time. Two different schemes are used for time differencing. In three dimensions, we use the second-order Adams–Bashforth scheme with a second-order Runge–Kutta scheme for the first time step. In two dimensions, we use a second-order Runge–Kutta scheme all along the integration.

Discretization of space. We use a finite-difference method with the same mesh size in all directions. We use second-order accurate differencing in three dimensions and fourth-order in two dimensions. At interior grid points, $\partial^2_{\xi_i}$ and ∂_{ξ_i} are computed by centered schemes. When derivatives at the boundary are needed, we use polynomial extrapolation to fictitious points outside the domain.

Evaluation of ξ integrals. We use Simpson's method to calculate the integrals in A given by (2.12) and in β given by (2.10) over the domain $\mathcal{N}=[-M, M]^d$. The choice $p \geq 3$ insures that for the values $M = 10$ or 20 we used, the integrands at the boundary are small enough to be set to zero.

Initial condition for u, λ, x_0 and the Euler angles. As we indicated before, given $\psi_0(x)$ the point x_0 is computed from (2.4) and the matrix S from (2.7) and (2.4). In the decomposition $S = O^T \Lambda^2 O$ we compute O and Λ^2 using the Eispack routines. We then have $D(0) = O^T(0)\Lambda(0)$ and $u_0(\xi)$ is computed from (2.1). The Euler angles are determined by O.

Approximate boundary conditions. To get an approximate boundary condition, we note that for ξ large enough, Δu and $|u|^2 u$ in (2.22) are negligible compared to the other terms so that, near the boundary of the domain, the transformed NLS reduces to

$$u_\tau - \frac{L_\tau}{L} u + f \cdot \nabla u = 0. \tag{3.1}$$

This equation is easily discretized when using a second-order Adams–Bashforth or Runge–Kutta scheme in time, with the gradient computed by a second-order polynomial extrapolation. However, this approximation will be good only if the solution at a point of the boundary at a given time is not influenced by the solution outside the domain at previous times. To see this more clearly, we solve eq. (3.1) explicitly after noting that it can be rewritten as

$$\left(\frac{u}{L}\right)_\tau + f \cdot \nabla\left(\frac{u}{L}\right) = 0.$$

This is a first-order partial differential equation that can be solved by the method of characteristics. The characteristics are

$$\frac{d\xi}{d\tau} = f \equiv -D^{-1}\frac{dD}{d\tau}\xi - D^{-1}\frac{dx_0}{d\tau},$$

which we rewrite as

$$D^{-1}(D\xi)_\tau = -D^{-1}(x_0)_\tau,$$

or

$$(D\xi + x_0)_\tau = 0. \tag{3.2}$$

This integrates to

$$\xi(\tau_1) = D^{-1}(\tau_1)\{D(\tau_2)\xi(\tau_2) + [x_0(\tau_2) - x_0(\tau_1)]\} \quad \text{for } \tau_2 > \tau_1, \tag{3.3}$$

and the solution of (3.1) is

$$\frac{u(\tau_2, \xi(\tau_2))}{L(\tau_2)} = \frac{u(\tau_1, \xi(\tau_1))}{L(\tau_1)}. \tag{3.4}$$

Assume that $u(\tau)$ and $L(\tau)$ are known from previous computations for $\tau < \tau_2$ in the domain $\mathcal{N}$, we then need an approximate value for u at a point η on the boundary of $\mathcal{N}$. We have from (3.4)

$$u(\tau_2, \eta) = \frac{L(\tau_2)}{L(\tau_1)} u(\tau_1, \xi(\tau_1)), \tag{3.5}$$

where

$$\xi(\tau_1) = D^{-1}(\tau_1)\{D(\tau_2)\eta + [x_0(\tau_2) - x_0(\tau_1)]\} \quad \text{for } \tau_2 > \tau_1. \tag{3.6}$$

In numerical calculations, when $\delta\tau = \tau_2 - \tau_1$ is small, the value $u(\tau_1, \xi(\tau_1))$ is approximated by the values near the boundary at τ_1. The time stepping is done by a second-order scheme. For example, when an Adams–Bashforth scheme is used, we have

$$u(\tau_2, \eta) = u(\tau_1, \eta) + \delta\tau \cdot \frac{1}{2}\left[3\left(\frac{L_\tau}{L}u - f\cdot\nabla u\right)(\tau_1, \eta) - \left(\frac{L_\tau}{L}u - f\cdot\nabla u\right)(\tau_1 - \delta\tau, \eta)\right]. \tag{3.7}$$

If $u(\tau_1, \xi(\tau_1))$ is outside the domain $\mathcal{N}$, then (3.7) is not a good approximation because we have no information outside $\mathcal{N}$. In our calculations this is not the case most of the time. A fixed domain $\mathcal{N}$ corresponds to a physical domain that is shrinking around the singular point if the scaling factors are decreasing, which is the case after an initial transient.

Note that in the case of radially symmetric solutions, (3.5) and (3.6) give the value of u at a given time at any point outside the integration domain in terms of its value on the boundary at a previous time. This can be used to compute the contribution to the L^2-norm of the solution coming from the region outside the integration domain. In ref. [9] this is used to check the conservation of this norm during the numerical integration. It cannot be extended to the multi-dimensional case.

4. Numerical results

In this section, we will present the numerical results we obtained by solving the nonlinear Schrödinger equation with anisotropic initial conditions.

In all the runs reported here p is taken to be 3 and the domain is taken to be $\mathcal{N} = [-M, M]^3$ with the approximate boundary condition discussed in section 3.

4.1. Three-dimensional (supercritical) case

Several computations were performed. We first tested the method and its accuracy by considering the radially symmetric initial condition $\psi_0 = 6\,e^{-(x^2+y^2+z^2)}$ which was extensively considered in refs. [3, 4]. Initially, $\lambda_1(0) = \lambda_2(0) = \lambda_3(0) = L(0) = 0.2887$. We have three runs with $M = 10$ and mesh sizes $h = 0.5$, $h = 0.333$ and $h = 0.25$ corresponding respectively to 40^3, 60^3 and 80^3 points for the spatial grid. The time step $\delta\tau$ is always chosen so that $\delta\tau/h^2 = 3/128$.

The computation shows that the λ_i stay indeed equal and so do the a_{ii}. After $\tau = 10$, the diagonal coefficient $a_{ii}(\tau) = a(\tau)$ of the matrix A and the τ-derivative, $c(\tau)$, of the phase of u at the origin, become nearly constant; the amplitude $|u|$ converges to a limit function. Our results clearly show convergence of the calculations as we refine the grids. For example, we calculate the $K = a/c$ values at $\tau = 15$ for various mesh sizes. We get $K = 0.9421$ for $h = 0.5$, $K = 0.9328$ for $h = 0.333$ and $K = 0.9240$ for $h = 0.25$, while the expected value is $K = 0.9173\ldots$. Therefore, the errors $e = K - 0.9173$ are $e = 0.10h^2$ for $h = 0.5$, $e = 0.14h^2$ for $h = 0.333$ and $e = 0.10h^2$ for $h = 0.25$, which is consistent with the second-order accuracy of the difference scheme. The profiles $|u(\xi_1, 0, 0)|$, $|u(0, \xi_2, 0)|$ and $|u(0, 0, \xi_3)|$ are identical and fit the Q profile of eq. (1.3) very well, especially when $h = 0.25$.

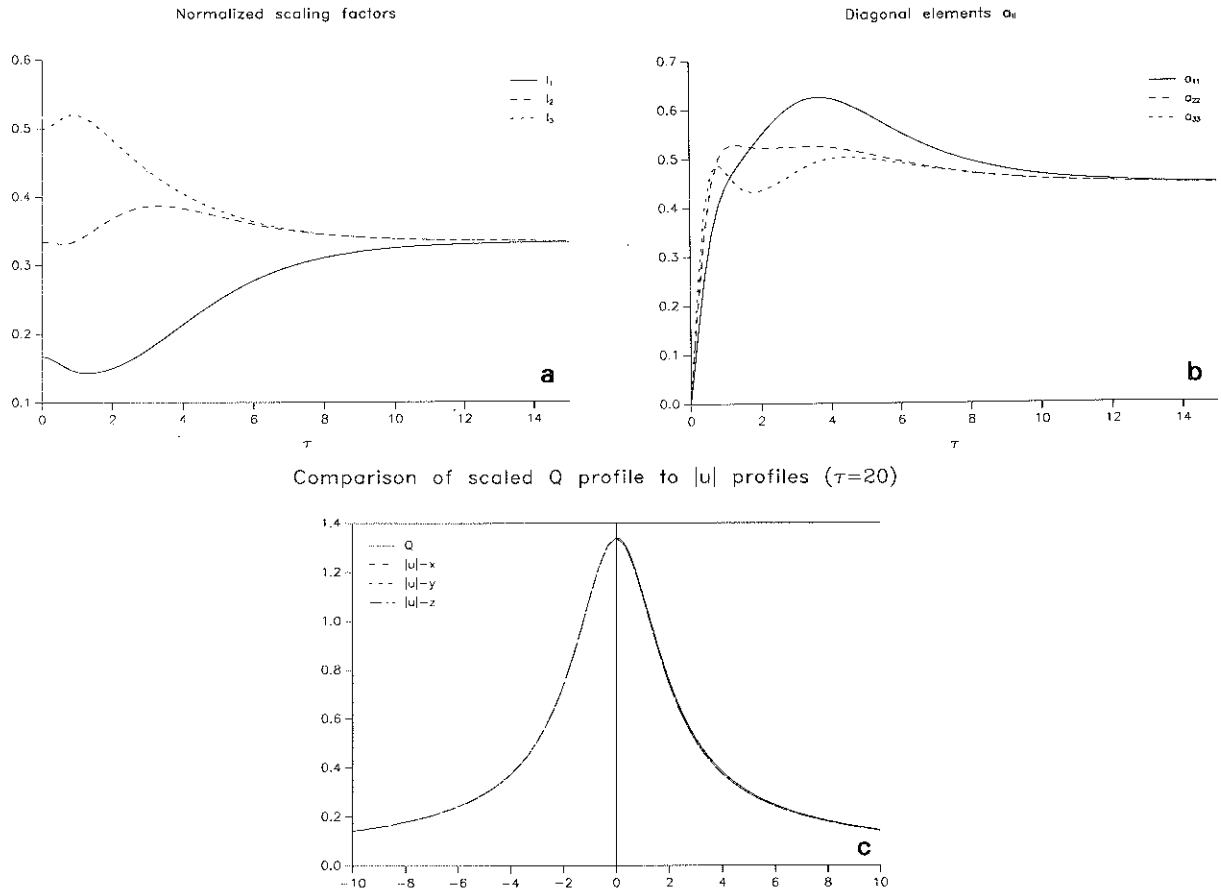

Fig. 1. Supercritical case ($d = 3$), initial data $\psi_0 = 6\,e^{-(x^2+2y^2+3z^2)}$. (a) Normalized scaling factors l_1, l_2, l_3 versus time τ. (b) Diagonal elements of matrix A versus time τ. (c) Q and $|u|$ profiles at time $\tau = 20$.

To see how the size of the computational domain (i.e. the M) affects the results we also have a run with a bigger domain $M = 15$ in the case $h = 0.5$. We found that K is 0.9412, which is a small improvement. It also shows that by restricting the computation to a finite domain we did not loose much accuracy in the evaluation of the integrals.

As a simple example of anisotropic initial condition, we choose $\psi_0 = 6\,e^{-(x^2+2y^2+3z^2)}$ for which $\lambda_1(0) = 0.2887$, $\lambda_2(0) = 0.2041$, $\lambda_3(0) = 0.1667$. With 60^3 grid points, and $M = 10$, we find that as $\tau \to \infty$, the normalized scaling factors $l_i = L^2/3\lambda_i^2$ all tend to $1/3$ and rapidly approach each other (fig. 1a). The diagonal elements of the A-matrix converge to the same finite value, while the off-diagonal elements tend to zero (fig. 1b). The graph of profiles $|u|$ along the three axes shows clearly that it becomes isotropic and fits the Q profile defined by (1.3) very well (fig. 1c). The phase at the origin is linear in τ and we get the limit value $K = 0.9306$, which is comparable to what we got in the radial case when using the same spatial resolution.

We also considered an example of initial condition displaying a stronger anisotropy, namely $\psi_0 = 6\,e^{-(x^2+y^2/4+z^2/8)}$ for which $\lambda_1(0) = 0.2887$, $\lambda_2(0) = 0.5774$ and $\lambda_3(0) = 0.8165$. We observed an early transient during which the anisotropy is significantly amplified, eventually the solution becomes isotropic.

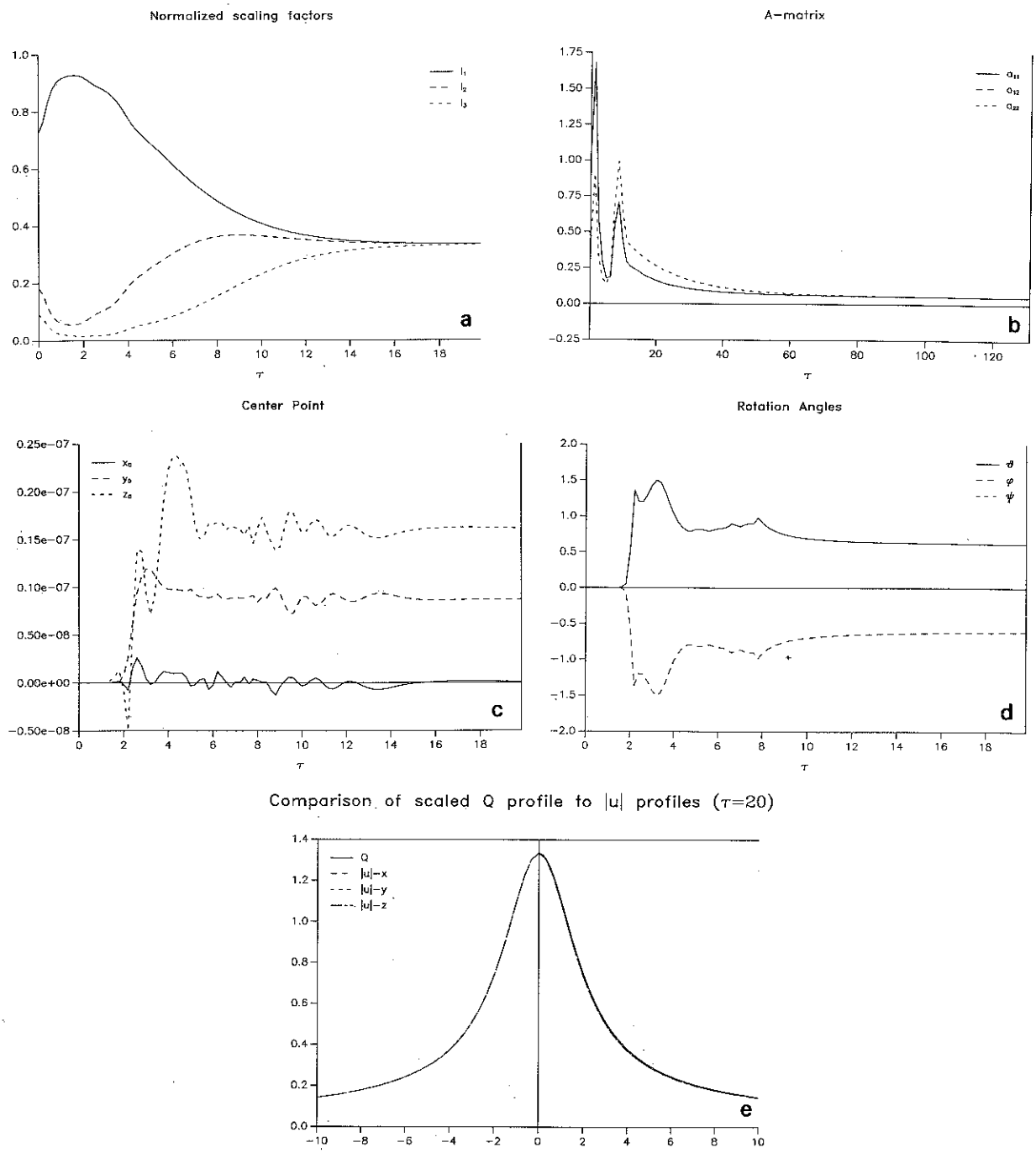

Fig. 2. Supercritical case ($d = 3$), initial data $\psi_0 = 6\,e^{-(x^2+y^2/4+z^2/8)}$. (a) Normalized scaling factors l_1, l_2, l_3 versus time τ. (b) Diagonal elements of matrix A versus time τ. (c) Coordinates (x_0, y_0, z_0) of center point of $|\psi|^{2p}$ (blowup point) versus time τ. (d) Rotation angles θ, ϕ, ψ versus time τ. (e) Q and $|u|$ profiles at time $\tau = 20$.

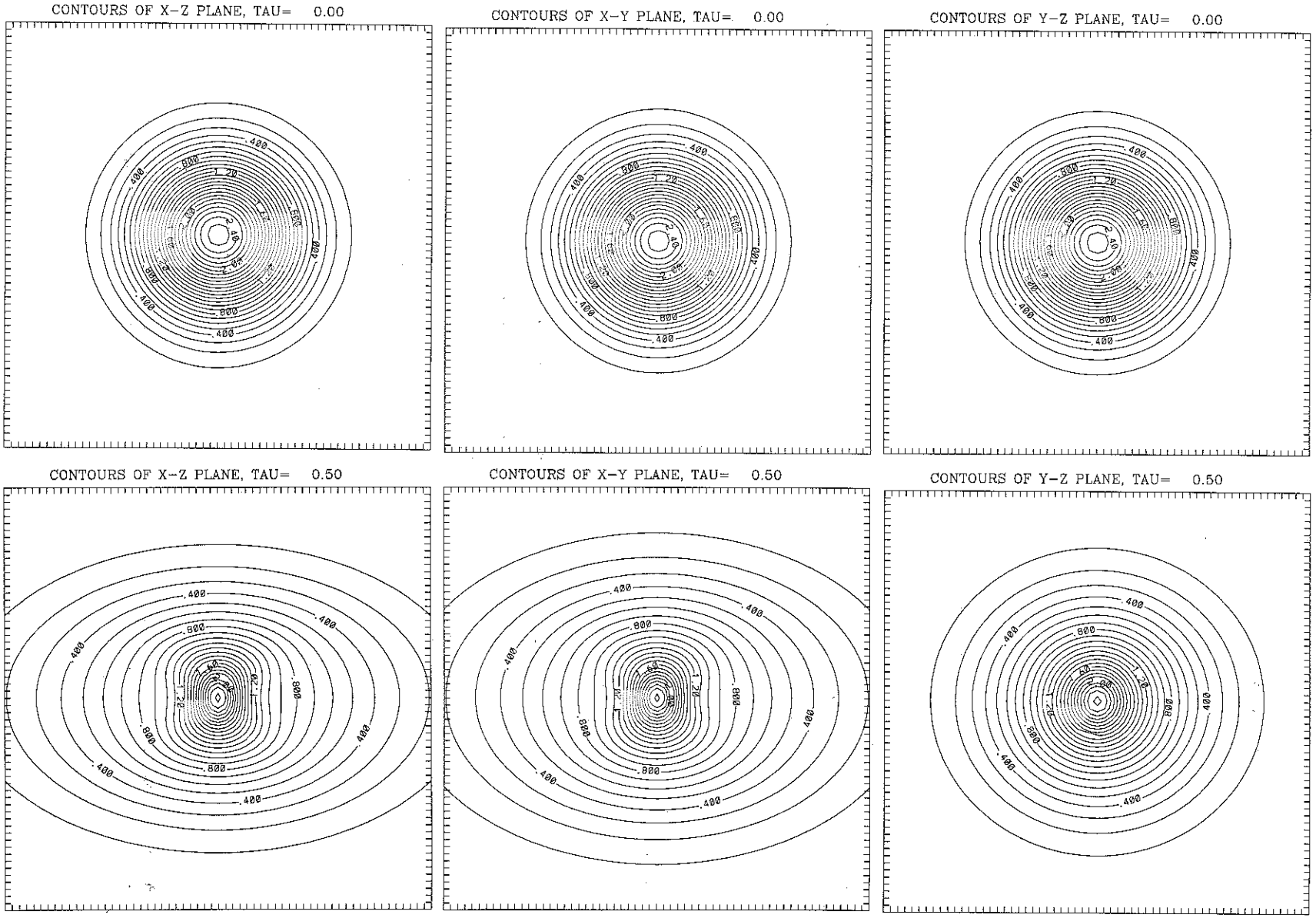

Fig. 3. Contours of $|u|$ in the planes $\xi_2 = 0$, $\xi_3 = 0$ and $\xi_1 = 0$ for initial data $\psi_0 = 6\,e^{-(x^2+y^2/4+z^2/8)}$ and $d = 3$ (supercritical case).

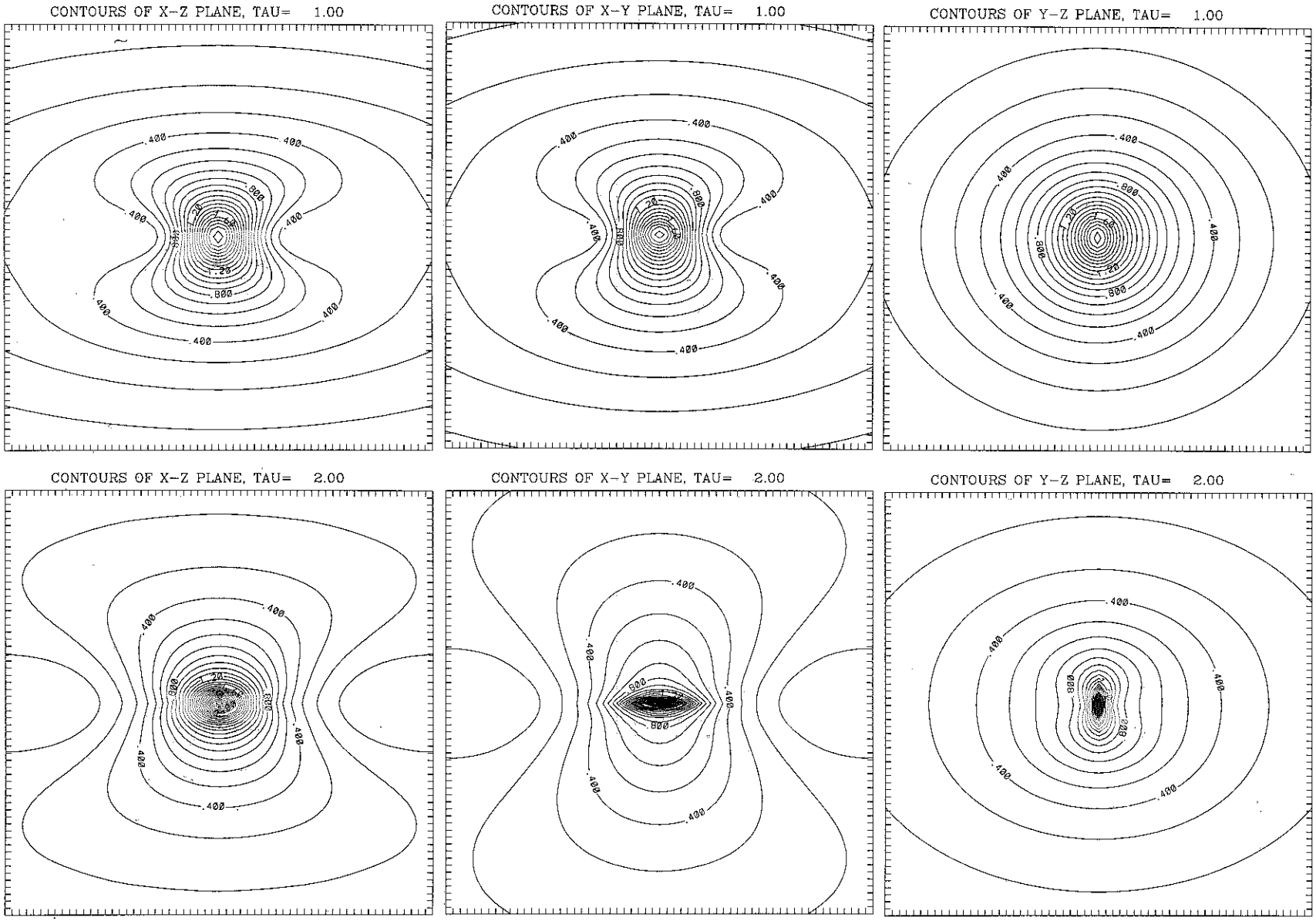

Fig. 3. Continued

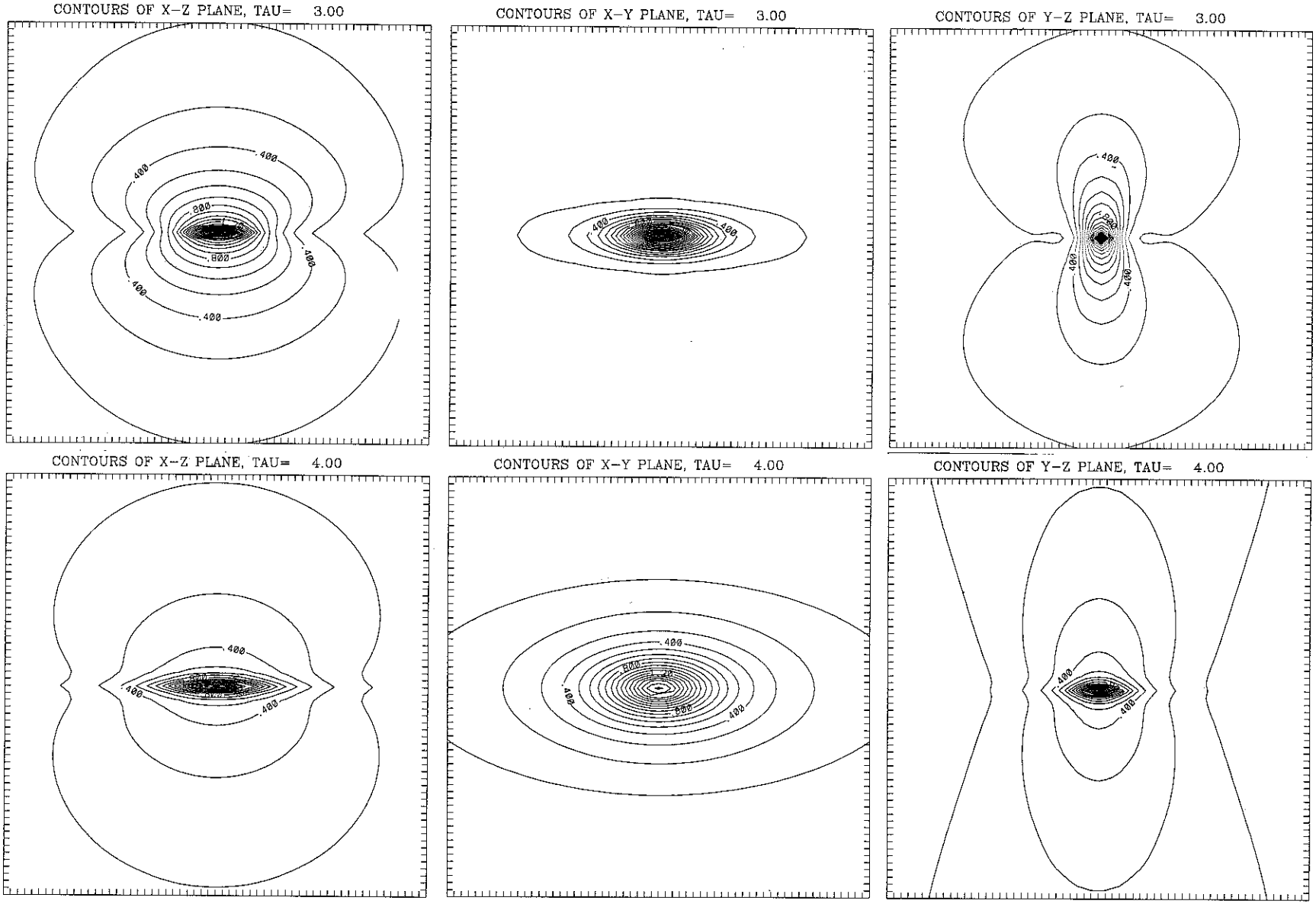

Fig. 3. Continued

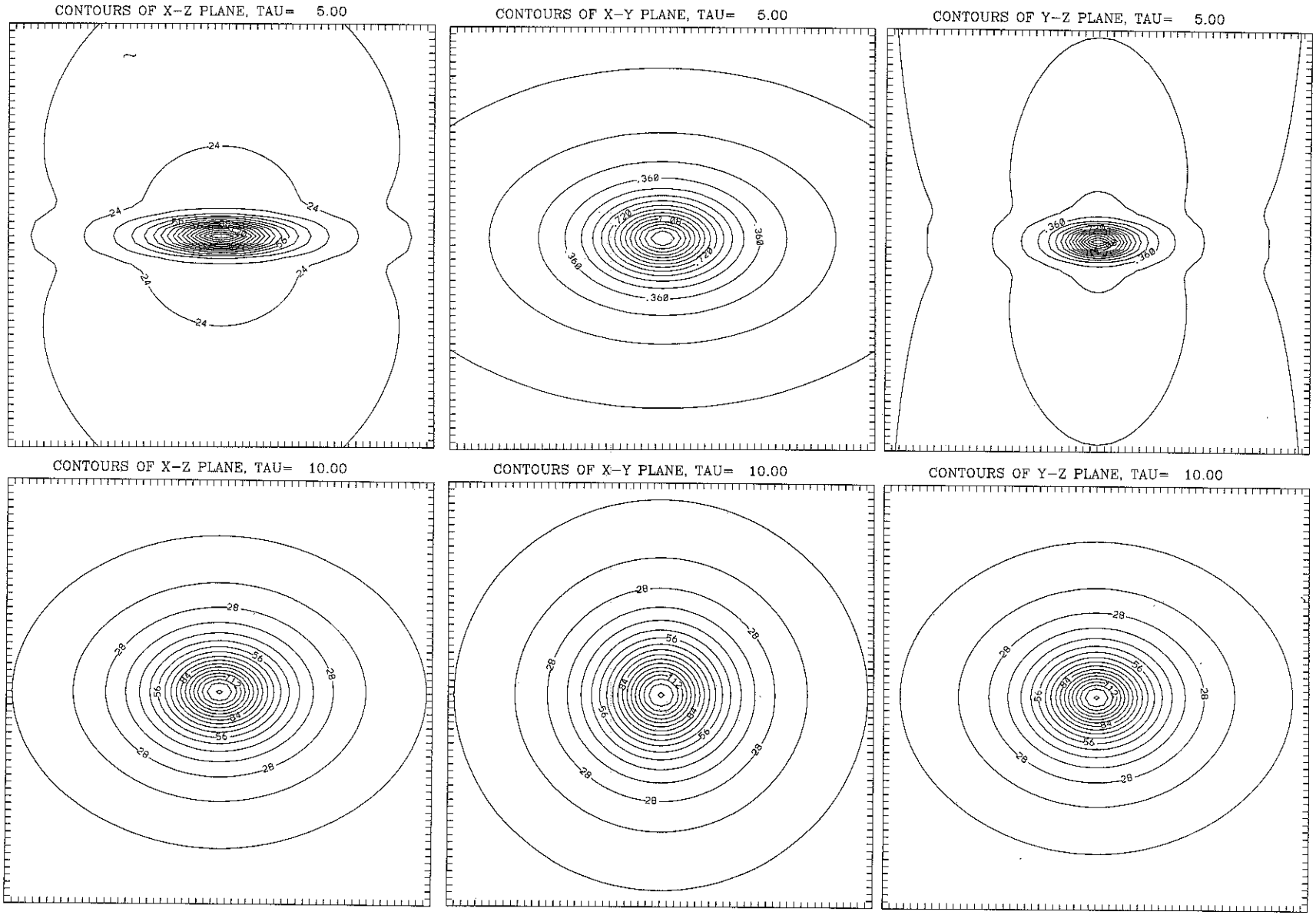

Fig. 3. Continued

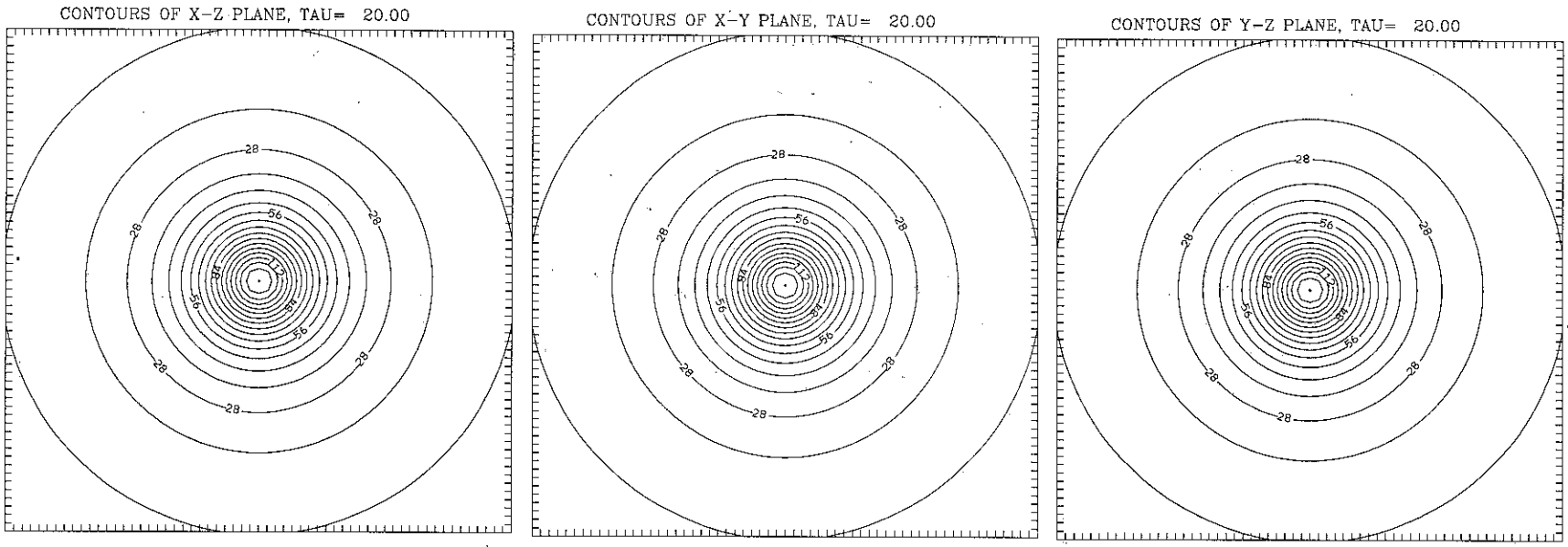

Fig. 3. Continued

This is illustrated in fig. 3 where contours of cross-sections of $|u|$ are plotted in the coordinate planes together with fig. 2a, which has the normalized scaling factors. We see that around $\tau = 2$ the contours in the $\xi = 0$ plane elongate in the ξ_3 direction and this is reinforced by the behavior of l_2 and l_3 which can be read from fig. 2a. Similar remarks hold for the contours in the $\xi_3 = 0$ plane, and in the $\xi_2 = 0$ plane, at an earlier time, around $\tau = 0.5$, although the anisotropy is not as sharp as in $\xi_1 = 0$ plane. Note that later the contours of $|u|$ become anisotropic in the opposite direction but because of the scaling factors the solution in the primitive variables is not so anisotropic. Figs. 2b–2e display other features of the solution: the evolution of the diagonal elements a_{ii}, the location of the blowup point, the rotation angles and the comparison of $|u|$ with the Q profile, respectively.

We also consider initial data corresponding to two different peaks, namely $\psi_0(x, y, z) = A\,e^{-(x+1)^2-y^2-z^2} + B\,e^{-(x-1)^2-y^2-z^2}$. We again used $M = 10$ and 40^3 grid points. We found that if one peak is higher than the other, for example $A = 6$ and $B = 3$, then the higher peak becomes stronger and eventually the lower one is absorbed by the higher one, leading to a single isotropic peak with an amplitude $|u|$ approaching the Q profile. Again we find that as $\tau \to \infty$, l_1, l_2 and l_3 approach each other very fast and tend to $\frac{1}{3}$. The diagonal elements of the A-matrix converge to the same finite limit value, with the off-diagonal elements tending to zero. In this example, the centroid x_0 moves during early transient and significant rotations of the solution are visible before an isotropic configuration is reached. Note that at early time, x_0 is located somewhere between the peaks. Since this occurs before significant focusing took place, it does not lead to loss of accuracy. When the solution has been significantly amplified, the stronger peak has already absorbed the weaker one and x_0 is correctly located at the focusing point. When however, the two peaks are equal, they stay away from each other and the solution collapses around each one. The nature of the collapse cannot be analyzed by the present method.

4.2. *Two-dimensional (critical) case*

As already observed in the calculation of radially symmetric solutions in refs. [4, 5], the critical case $d = 2$ is characterized by a slowing down of the dynamics and the integration has to be carried out to a much longer time than in three dimensions in order to reach the asymptotic regime. Here we use a

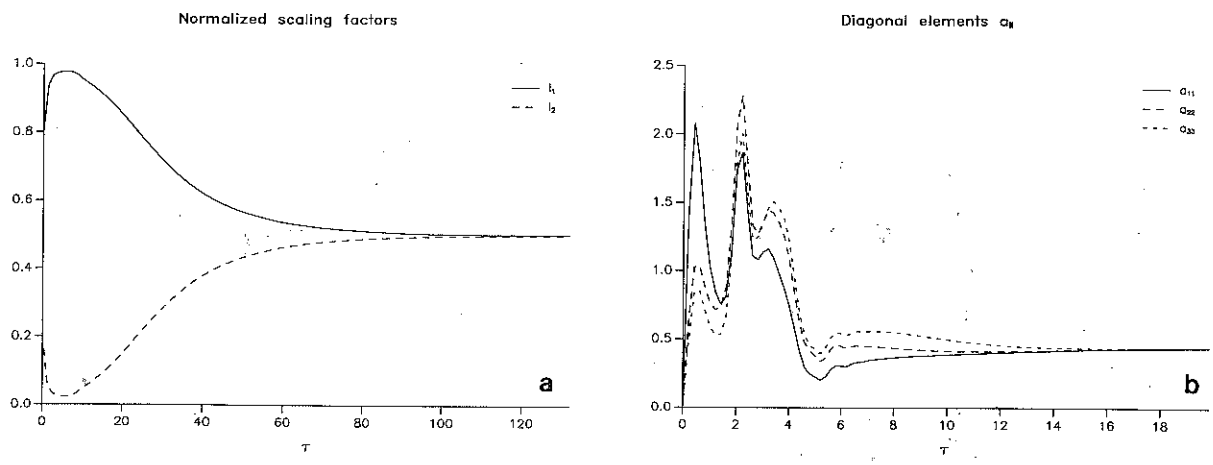

Fig. 4. Critical case ($d = 2$), initial data $\psi_0 = 2.5\,e^{-(x^2+y^2/4)}$. (a) Normalized scaling factors l_1, l_2 versus time τ. (b) Matrix A versus time τ.

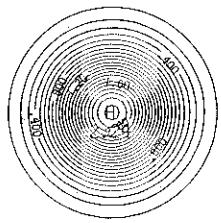

TAU = 0.000

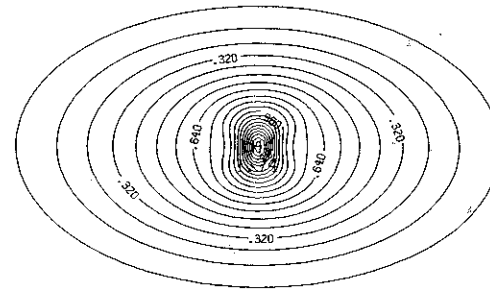

TAU = 1.000

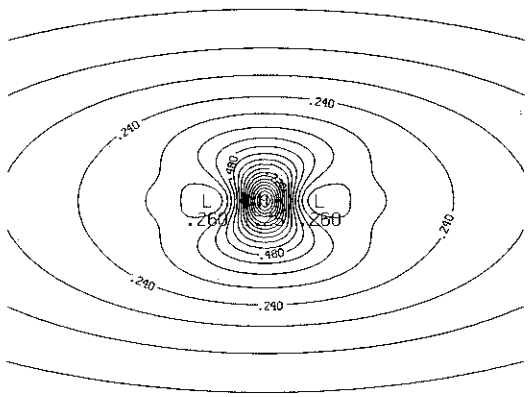

TAU = 2.000

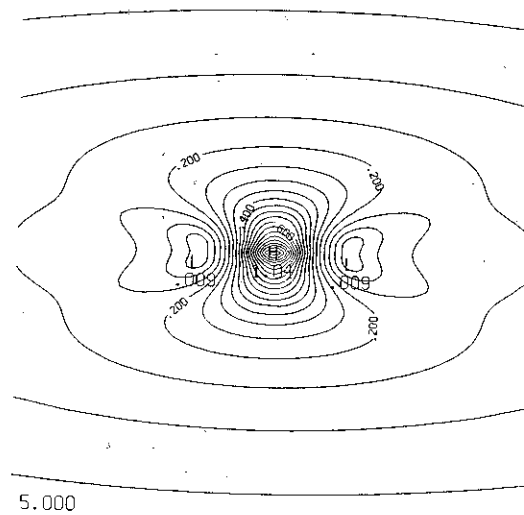

TAU = 5.000

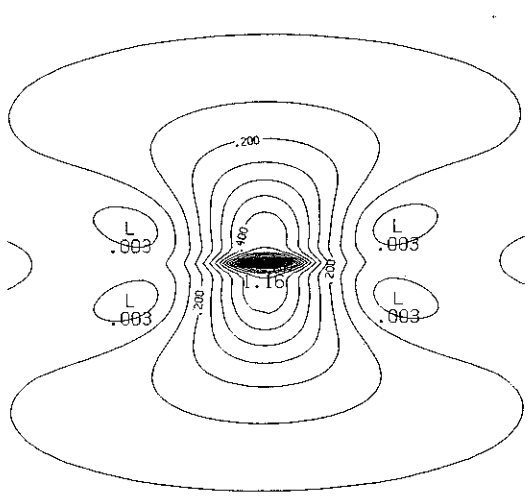

TAU = 8.000

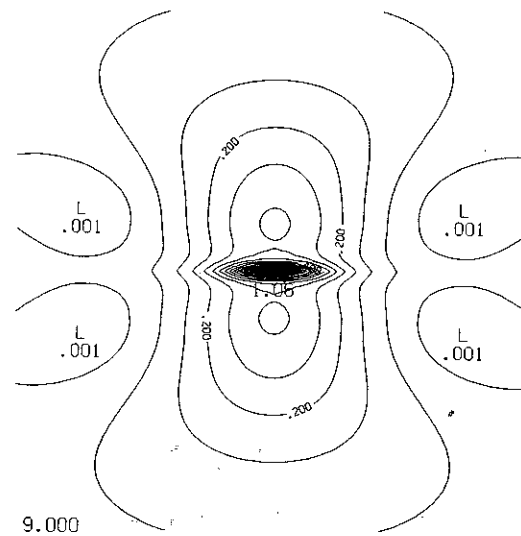

TAU = 9.000

Fig. 5. Contours of $|u|$ at various times τ.

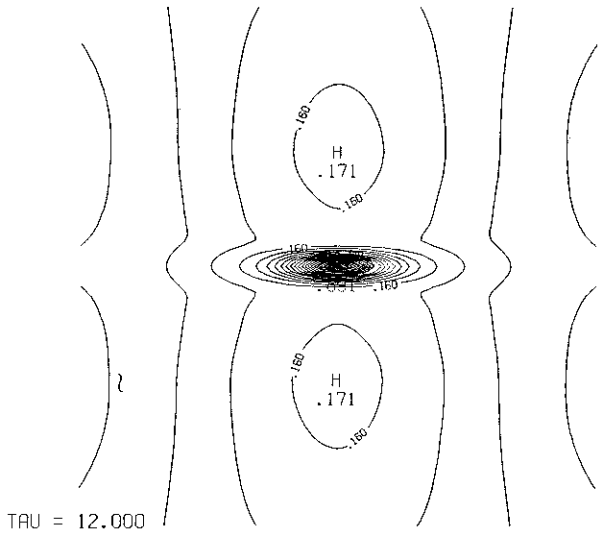

TAU = 12.000

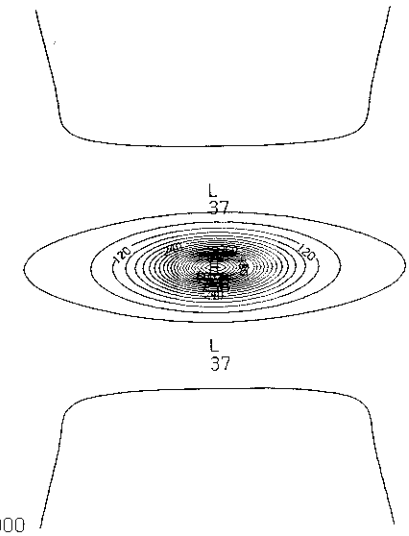

TAU = 19.000

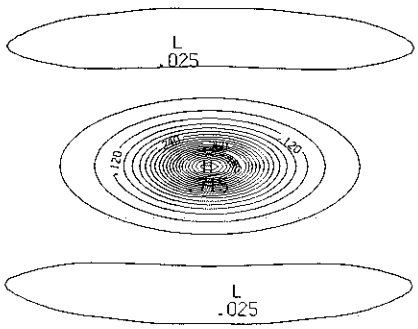

TAU = 23.000

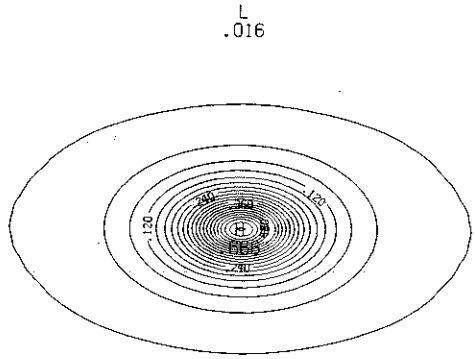

TAU = 29.000

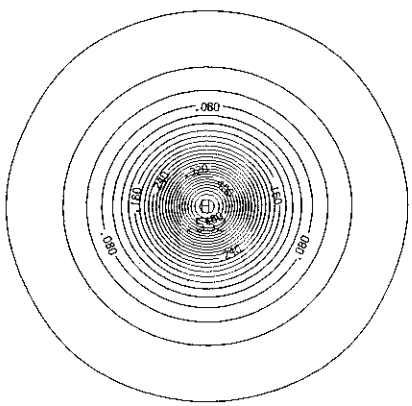

TAU = 66.000

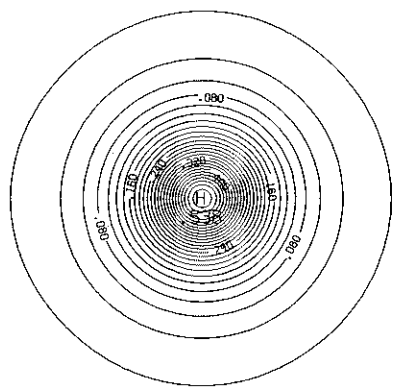

TAU =100.000

Fig. 5. Continued

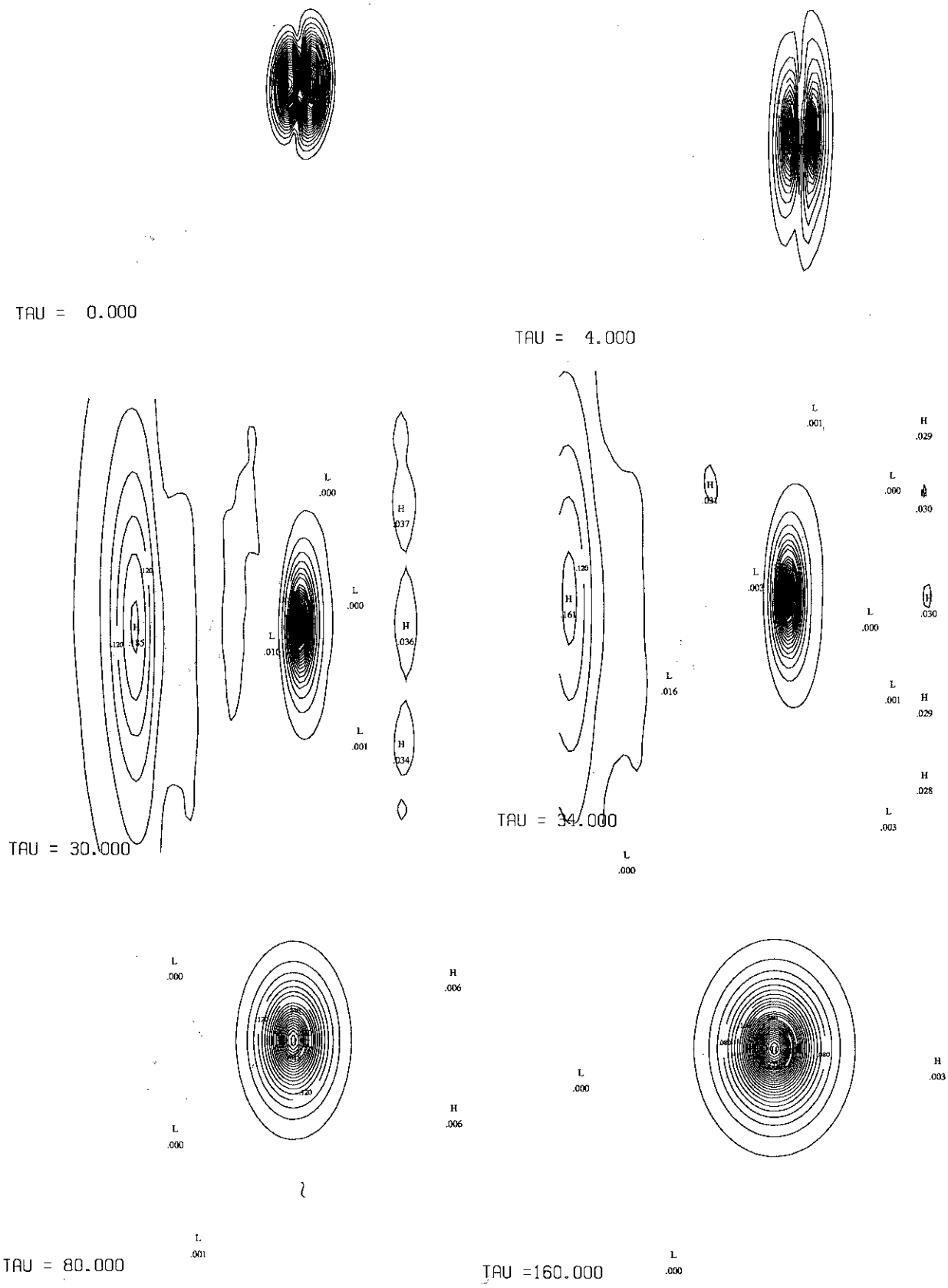

Fig. 6. Contours of $|u|$ at various times τ. Critical case ($d = 2$), initial data $\psi_0 = (x^2 + x + 3y)\mathrm{e}^{-(x^2+y^2/4)}$.

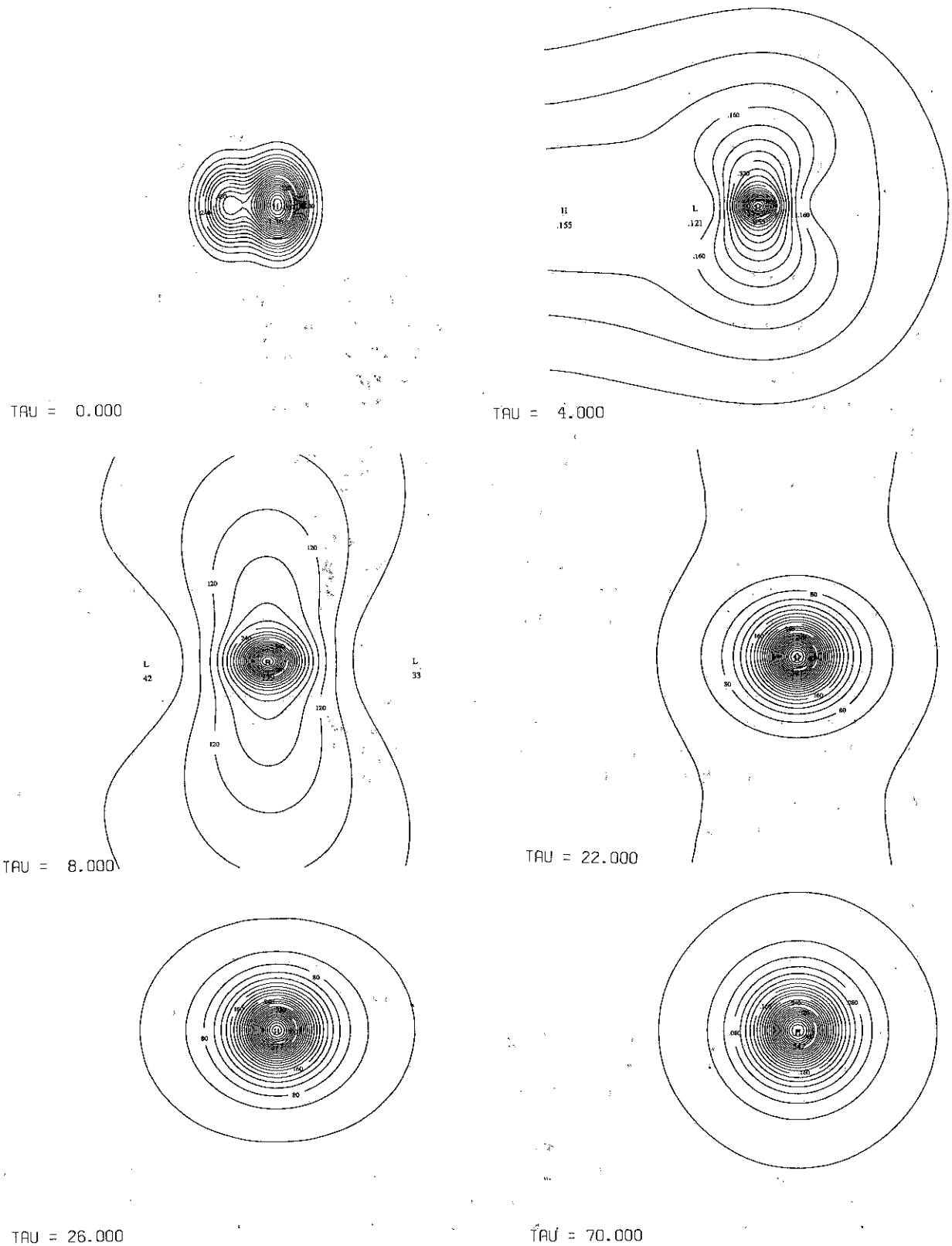

Fig. 7. Contours of $|u|$ at various times τ. Critical case ($d = 2$), initial data $\psi_0 = 4\,e^{-[(x-1)^2+y^2/4]} + 2\,e^{-[(x+1)^2+y^2/4]}$.

resolution of 100^2 grid points in a domain with $M = 15$ or 20 and with a time step $d\tau = 10^{-3}$. Again the code was checked by considering radially symmetric initial conditions and comparing with ref. [4].

We integrated eqs. (2.22) and (2.23) with various anisotropic initial conditions, all satisfying the requirement for blowup. As a simple example, we took the initial condition I_1: $\psi_0 = 2.5\, e^{-(x^2+y^2/4)}$. Because of symmetry, the singularity stays at the origin. After rescaling the initial condition u_0 is isotropic. Initially, the normalized scaling factors $l_i = L^2/2\lambda_i^2$ are initially different, like in three dimensions, the anisotropy is strongly amplified during an early transient. Later, the l_i's approach each other and when τ goes to infinity they both tend to $1/2$ (fig. 4a). The evolution of the coefficients a_{11} and a_{22} of the A-matrix is shown in fig. 4b. In the present example, $a_{12} = a_{21} = 0$ by symmetry. When τ goes to infinity, a_{11} and a_{22} approach to each other and, as expected in dimension two, tend to 0 very slowly. Figs. 5a, 5b show the contours of $|u(\xi, \tau)|$ at various (rescaled) times. After a transient period we see clearly the relaxation to an isotropic shape. Together with the convergence of l_1 and l_2 to $\frac{1}{2}$, this implies that in the primitive variables the solution displays a radially symmetric structure near the singularity.

Similar results were obtained with an initial condition like (I_1), except that a phase linear in x and y is added.

We also considered an initial condition displaying several local maxima I_2: $\psi_0 = (x^2 + x + 3y)\, e^{-(x^2+y^2/4)}$. We find that when τ goes to infinity, the rescaled factors l_1 and l_2 tend to different values 0.347 and 0.654, respectively. This, however, does not imply anisotropy of the singularity in the primitive variables. Indeed, fig. 6 shows contours of the rescaled profiles $|u(\xi, \tau)|$ at various times. We see that they display complicated shapes at moderate τ. However, when τ tends to infinity they tend to a family of ellipses whose axes are precisely in the ratio $\sqrt{l_2/l_1}$. Coming back to the primitive variables, we see that ψ blows up with an isotropic local structure. Again, the coefficients of the A-matrix tend slowly to zero.

In order to see how two peaks compete to form singularities we considered the initial condition I_3: $\psi_0 = 4\, e^{-[(x-1)^2+y^2/4]} + 2\, e^{-[(x+1)^2+y^2/4]}$. As in three dimensions, we observe that the higher peak becomes stronger and eventually the lower peak is absorbed by a higher one leading to a unique isotropic singularity (fig. 7). Since the normalized scaling factors converge both to the same value of 0.5, we conclude again that the physical solution is isotropic near the singularity.

When the two peaks are equal we found initially, as in three dimensions, that the solution blows up around two distinct points.

5. Conclusions

We have extended the method of dynamic rescaling introduced in ref. [4] to the case of anisotropic solutions of the nonlinear Schrödinger equation. In full two- and three-dimensional computations we find that when solutions blow up at one point, near that point they have the isotropic structure found numerically in refs. [4, 5] and studied analytically in refs. [10–12]. We conclude therefore that these isotropic singular solutions are dynamically stable for a broad class of initial conditions that lead to a singularity at only one point. Multi-point singularities cannot be studied by the method of this paper.

There is no analytical understanding of the stability of isotropic singular solutions in the supercritical ($d > 2$) or critical ($d = 2$) case for the nonlinear Schrödinger equation.

Anisotropic singular solutions have been constructed in refs. [16, 17] and physical arguments have been given that indicate that such solutions, and not the isotropic ones, are dynamically stable. In our computations we have found examples of both three- and two-dimensional solutions (figs. 3 and 5) which

go through a strongly anisotropic stage before settling eventually to the isotropic form near the singula point. A less accurate computation that could not get the solution so close to the singularity, might hav stopped in the transient stage leading to a wrong conclusion concerning the form of the singularity.

We do not know if the isotropic singular solutions are also structurally stable for physically interestin perturbations of the nonlinear Schrödinger equation. It may turn out that anisotropic singular solution become stable under such perturbations. This question is being studied at present.

Acknowledgements

We thank V.E. Zakharov for providing us a preprint of ref. [9] and for bringing to our attention th work of Fraiman [13]. This work was supported by the National Science Foundation (DMS-8701895) an by the Air Force Office of Scientific Research (AFOSR 86-0352).

References

[1] A.C. Newell, Solitons in Mathematics and Physics, CBMS Applied Mathematical Series, Vol. 48 (SIAM, Philadelphia, 1985)
[2] V.E. Zakharov, Zh. Eksp. Theor. Fiz. 18 (1972) 1745; Sov. Phys. JETP 35 (1972) 908.
[3] R.T. Glassey, J. Math. Phys. 18 (1977) 1974.
[4] D.W. McLaughlin, G. Papanicolaou, C. Sulem and P.L. Sulem, Phys. Rev. A 34 (1986) 1200.
[5] B. LeMesurier, G. Papanicolaou, C. Sulem and P.L. Sulem, Physica D 31 (1988) 78.
[6] D.B. Budneva, V.E. Zakharov and V.S. Synakh, Fiz. Plasma, 1 (1975) 606; Sov. J. Plasma Phys. 1 (1975) 335.
[7] M.V. Goldman, K. Rypdal and B. Hafizi, Phys. Fluids 23 (1980) 945.
[8] V.E. Zakharov, Collapse of self-focusing of Langmuir waves, in: Handbook of Plasma Physics, Vol. 2, eds. M.N. Rosenbluth and R.Z. Sagdeev (North-Holland, Amsterdam, 1984).
[9] N.E. Kosmatov, I.V. Petrov, V.F. Shvets and V.E. Zakharov, Large amplitude simulation of wave collapse in nonlinear Schrödinger equations, Academy of Sciences of the USSR, Space Research Institute, Preprint (1988);
V.E. Zakharov and V.F. Shvets, JETP Lett. 47 (1988) 275;
V.E. Zakharov, A.G. Litvak, E.N. Rakova, A.M. Sergeel and V.F. Shvets, Sov. Phys. JETP 67 (1988) 925;
V.E. Zakharov, N.E. Kosmatov and V.F. Shvets, JETP Lett. 49 (1989) 432.
[10] B. LeMesurier, G. Papanicolaou, C. Sulem and P.L. Sulem, Physica D 32 (1988) 210.
[11] M. Landman, G. Papanicolaou, C. Sulem and P.L. Sulem, Phys. Rev. A 38 (1988) 3837.
[12] M. Landman, G. Papanicolaou, C. Sulem and P.L. Sulem, in: Integrable Systems and Applications, eds. M. Balabane P. Lochak and C. Sulem, Lecture Notes in Physics 342 (Springer, Berlin, 1989) p. 207.
[13] G.M. Fraiman, Zh. Eksp. Theor. Fiz. 88 (1985) 390; Sov. Phys. JETP 61 (1986) 228.
[14] P.L. Sulem, C. Sulem and A. Patera, Comm. Pure Appl. Math. 37 (1986) 755.
[15] V.E. Zakharov and E.A. Kuznetsov, Zh. Eksp. Theor. Fiz. 68 (1975) 115; Sov. Phys. JETP 64 (1986) 773.
[16] G. Pelletier, Physica D 27 (1987) 187.
[17] L.M. Degtyarev and V.E. Zakharov, Zh. Eksp. Theor. Fiz. Pis'ma Red. 20 (1974) 365; JETP Lett. 20 (1976) 16.
[18] P.A. Robinson, D.L. Newman and M.V. Goldman, Phys. Rev. Lett. 61 (1988) 2929.